Published in *Comments on Astrophysics*, 1993, Vol. 16, No. 6, pp. 331-361

TOWARDS UNDERSTANDING ACTIVE GALACTIC NUCLEI

F. H. Wallinder

ABSTRACT. Some selected aspects of current research into active galactic nuclei (AGN) are reviewed. Included topics are the continuum, the broad emission line region and the existence of black holes in galactic nuclei. It is found that an increasing number of observations indicates the presence of accretion disks around massive black holes.

Key Words: active galaxies, black holes, accretion disks, variability, broad line region

Table of Contents

Next

Next Contents

1. INTRODUCTION

During galaxy formation, a central condensation of mass emerged in the nuclei of most proto-galaxies, which in a majority of cases probably evolved into a supermassive black hole. A part of the remaining mass should then have had enough angular momentum to form an accretion disk in differential rotation around the black hole. Exactly how the gravitational energy is converted into radiation is unknown. The standard alternative is turbulent viscosity opposing the shear in the disk, producing heat radiation which is emitted from the disk surfaces. Another is dissipation in a hot, optically thin plasma exterior to the inner accretion disk. The resulting radiation should power several high-energy phenomena in active galactic nuclei (AGN), even though some energy may be extracted from the black hole rotation.

The combination of a disk and a supermassive black hole may thus be directly responsible for the observed continuum (Section 2), the ionization of clouds and line formation in the inner nucleus (Section 3) and possibly the formation of jets. As the matter supply to the nuclei decreased, AGN activity declined to the present-day low level.

The standard (circumstantial) arguments [1, 2] in favour of the above picture contain no conclusive evidence of either accretion disks or black holes in AGN. It could be that some of the recent developments discussed below will be able to change this situation.

In the following, some fiducial values of standard parameters will be needed. The radius of a Schwarzschild black hole is

$$r_g = \frac{2GM}{c^2} = 10^{-5} M_8 \text{ pc}, \qquad (1)$$

where G is the gravitational constant, c the speed of light and M_8 the central mass M in units of $10^8 M_\odot$. The light-crossing time corresponding to this radius is

$$t_g = \frac{2GM}{c^3} = 10^3 M_8 \text{ s}. \qquad (2)$$

Another fundamental parameter is the Eddington luminosity, given by

$$L_E = \frac{4\pi GM m_p c}{\sigma_T} = 10^{46} M_8 \text{ ergs}^{-1}, \qquad (3)$$

where m_p is the proton mass and σ_T the Thomson cross section for electron scattering. A spherical source with this luminosity has enough radiation pressure to balance the inward directed gravitational pull. One may subsequently define a critical accretion rate

$$\dot{M}_c = \frac{\dot{M}_E}{\varepsilon} = \frac{L_E}{\varepsilon c^2} = \frac{2M_8}{\varepsilon_{0.1}} M_\odot \ \mathrm{yr}^{-1}, \qquad (4)$$

where $\dot{M}_E$ is the Eddington accretion rate and $\varepsilon_{0.1} = \varepsilon / 0.1$ the scaled accretion efficiency. This leads to the dimensionless accretion rate $\dot{m} \equiv \dot{M} / \dot{M}_c = L / L_E$, which measures the total disk luminosity in terms of the Eddington one.

Disks with $\dot{m} << 1$, ~ 1 and $>> 1$ are referred to as thin, slim and thick, respectively, which reflects the increase of vertical extent of the disk, as $\dot{m}$ increases. The thickening results from the corresponding growth of internal pressure. Many AGN seem to accrete at a rate $\dot{m} \sim 1$ (Fig. 1), implying that the standard Shakura and Sunyaev [3, 4] thin disk model does *not* provide a relevant description of the inner region, where most of the gravitational energy is released. An increasing number of observational arguments has also diminished the relevance of the thin disk model. [6] The more appropriate slim disk models have been described in detail elsewhere. [7 - 10] Such disks are able to give a physically relevant description of the inner disk region, including effects like transonic radial motion, pressure, velocity and entropy gradients and non-Keplerian rotation. If stability properties (for instance, local instabilities) of such disks can be connected with observed variability patterns, it may be possible to constrain several rather fundamental parameters, such as the accretion rate and the central mass. Hence, the use especially of X-ray variability may provide the key to an increased understanding of the central engine, which in this context refers to radii between ~ 3 and $10^2\ r_g$ in the disk.

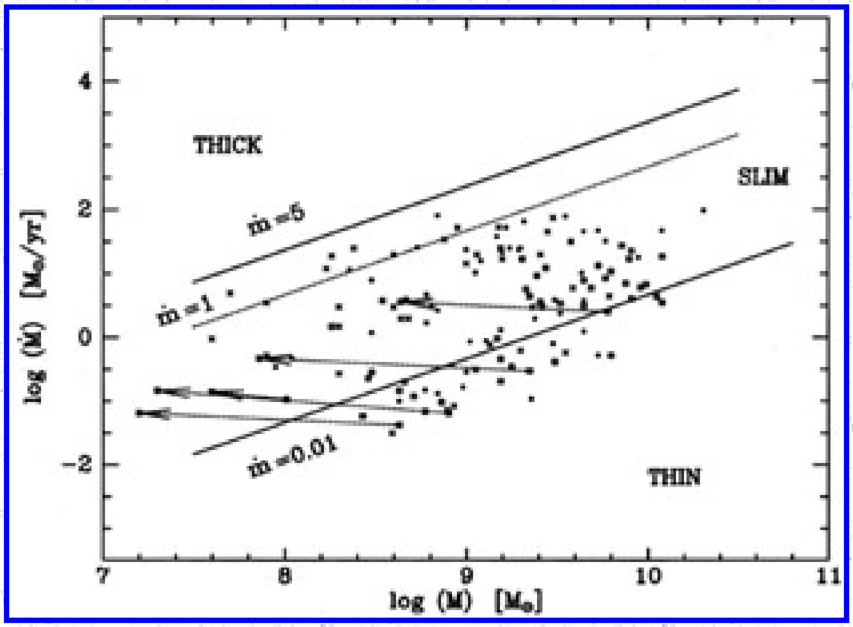

Figure 1. The relation between central mass *M* and accretion rate $\dot{M}$ in typical AGN. Adapted from Ref. 5.

Next Contents

2. THE CONTINUUM

The continuum emission is one of the primary channels by which AGN release energy. The physical understanding of the various mechanisms which give rise to the continuum is still rather rudimentary, and at least some of the proposed (textbook) explanations may lack relevance altogether. One significant step forward could be the growing number of multiwavelength, coordinated observational campaigns from observatories both on Earth and in space. In spite of this, the spectral coverage is at present far from complete, leaving the bolometric luminosity undetermined in many sources. The unobserved extreme UV (EUV) region is one particular example.

Non-blazar continuum spectra are often *assumed* to contain an underlying power law

$$F_{\nu} = K\nu^{-\alpha} \text{ ergs}^{-1}\text{ cm}^{-2}\text{ Hz}^{-1}, \qquad (5)$$

with a spectral index $\alpha \sim 1$, extending over a range of 10^4 in frequency (from IR to X-rays), on top of which various bumps are superposed. A generic AGN spectrum is given in Fig. 2.

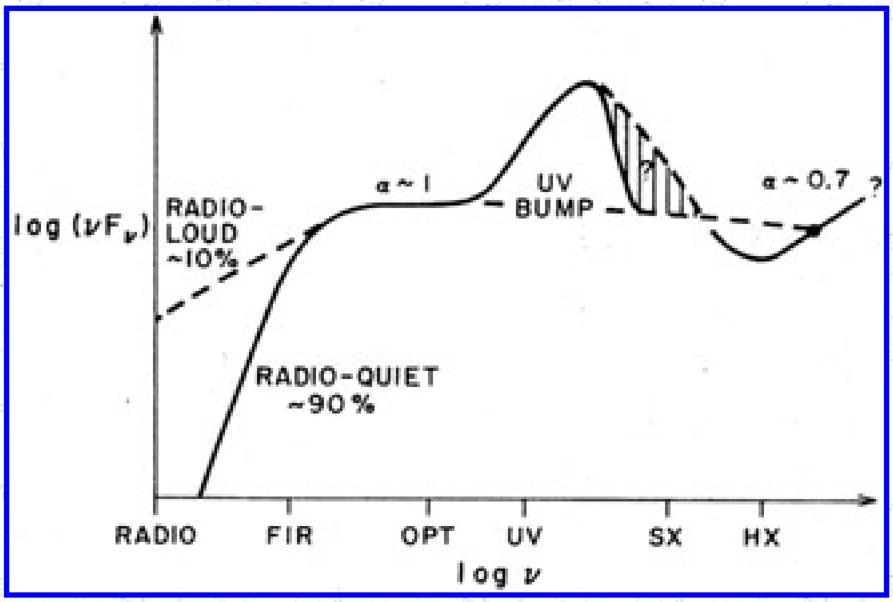

Figure 2. A typical AGN continuum (theorist's view). Consistency with the observed y-ray background implies another turnover at higher energies. From Ref. 11.

2.1 The IR Continuum

As can be seen in Fig. 2, the IR continuum contains in general two turnovers, one in the far infrared (FIR) at about 60 μm and another at ~ 1 μm. Observations by IRAS indicated no IR variability of radio-quiet AGN, at least on timescales less than a year. This may have ruled out Comptonized, self-absorbed thermal cyclotron radiation and self-absorbed synchrotron radiation [11] as the cause of the first turnover, since these mechanisms require a rather small source size. An increasing number of indications points towards dust heated by the central UV source as the origin of the IR continuum, even though a contribution from stars and cool dust in the host galaxy may be significant, especially in low-luminosity objects. [12] The combination of dust emission from the nucleus and the host galaxy emission can thus give rise to the quasi power law observed in some sources, without invoking any non-thermal mechanism. The turnovers could correspond to the minimum and maximum temperatures attainable by the dust grains. For instance, the short-wavelength one may be due to the onset of evaporation at about 1500 K. The dust hypothesis has gained additional support from studies of, e.g., ultraluminous IRAS galaxies [13] and flux ratios in IR. [14]

In the case of Seyfert 2s, the ionizing radiation seems to escape anisotropically. [15] An explanation due to a dusty obscuring torus seems preferable [16] to the anisotropic emission from the funnel of a thick accretion disk, [17] and is also consistent with the unified scheme for Seyfert galaxies. [18] One unexplained feature of this picture is the geometrical thickness of the torus. [19] Bregman [20] found that the IR-emission from essentially all radio-quiet AGN should have a thermal origin.

One particular example of reprocessing could be the radio-galaxy Cygnus A, where most of the total luminosity seems to be contained in a single spectral feature [21] with a temperature ~ 75 K. The absence of a strong UV-optical continuum in this and other similar sources may be due to dust absorption. The inferred intrinsic luminosity is in the quasar range, and the rest-frame extinction amounts to $A_V \backsimeq 50 \pm 30$ magnitudes. [22, 23]

An alternative obscuration scenario [24] involves a warped disk of gas and dust, possibly giving rise to most of the FIR and sub-mm continuum emission from radio-quiet AGN. However, the warp itself seems unexplained. [19]

2.2 The Optical-UV Continuum

The optical-UV feature in Fig. 2 is referred to as the ``big blue bump''. which in many sources contains a significant fraction of the bolometric luminosity. One possible origin is thermal emission from an accretion disk, [25] - [27] and spectral fits using disk spectra have the advantage of being able to estimate both the luminosity (accretion rate) and the central mass. However, a part of the UV bump may arise from reprocessing of radiation from the central hard X-ray source, which seems indicated by the similar variability patterns seen in UV, optical and X-rays. [28] This behaviour has only been observed in a few objects (such as NGC 5548), and it is unclear if the same applies to other sources with a lower X-ray luminosity. [29]

An alternative model, which involves dense, compact clouds with a high opacity, has been proposed by Guilbert and Rees [30] and independently by Lightman and White. [31] Located close to the central hard X-ray source, such clouds would emit thermal radiation, similar to the big bump. Collin-Souffrin [32] pointed out that since the X-ray and UV continua then would arise in the same physical region, the corresponding variability timescales should be approximately the same. This is not the case for at least high-luminosity AGN, where the X-ray fluctuations are more rapid. Moreover, the small total emitting surface of the clouds would imply a negligible UV luminosity in comparison with the bolometric one, which also is not observed.

Next Contents Previous

2.3 The X-ray Continuum

The short timescale of the X-ray variability in radio-quiet AGN indicates an origin in the central engine itself. Analyses of such data may therefore provide crucial insights into how the latter operates. The power contained in the X-ray band is typically ~ 30% of the estimated bolometric luminosity. [33]

Next Contents Previous

2.3.1 *The Soft Excess*

More than half of all Seyferts observed by EXOSAT showed an excess above the presumed underlying power law, in the range 0.1-2 keV. In fact, there is growing evidence of soft X-ray excesses being present in all AGN. [34] The excess has been connected with a high-energy tail of the UV bump, [35] but this suggestion awaits observational verification. Using the Shakura-Sunyaev model to fit the excess may be inappropriate, since a relevant temperature often requires $\dot{m} \gtrsim 1$. Another complication is that the disk should have a high inclination, [36] which implies an optical emission much fainter than for a face-on disk. However, sources with detected excesses show an optical emission typical of other AGN. [34]

The alternative origin due to Comptonization in a corona [37] may have been ruled out by the short variability timescale of the excess. [38] However, the mechanisms behind the excess and the hard X-rays may operate in approximately the same region, since their variability timescales are roughly similar, as observed [39, 40] in NGC 5548 and MCG-6-30-15. Possible mechanisms include Comptonization in an optically thin part of the accretion disk (next section) or a thermalized pair plasma. [41]

2.3.2 *The Hard X-ray Power Law*

Early X-ray observations [42] of mainly low-luminosity Seyfert 1 galaxies suggested that the spectra in hard X-rays (2-20 keV) in general conform to a power law with an index ~ 0.7. A lot of effort [43 - 46] has been devoted to ``explaining" this power law in terms of the so-called standard pair model, in which monoenergetic relativistic electrons are continuously injected into a spherical, homogeneous region, filled with soft photons. The electrons would produce γ-rays through inverse Compton scattering, which leads to pair production from photon-photon interactions involving the γ-rays. The pairs would then constitute a secondary injection, producing new pairs and so forth, resulting in a pair cascade. The latter is called saturated [45] if practically all the y-rays are reprocessed into hard X-rays, in which case the spectral index becomes ~ 1. This model failed because a relevant spectral index and the MeV break required by the observed γ-ray background could not be obtained. [47, 48]

Subsequent Ginga observations [49] revealed that the emission in the 1-30 keV range has a multicomponent structure, including an incident power law with a spectral index α^{int} ~ 0.9 and an excess above 10 keV. Zdziarski et al. [50] suggested that these features could be explained by the standard pair model, if hard X-rays from the pair plasma become Compton reflected in the inner disk. It is unclear whether the standard pair model can be saved in this way. One remaining concern is the connection to the environment, since the proposed physical scenarios seem oversimplified. In particular, both the coupling to a *physically relevant* accretion disk and various time-dependent effects warrant further investigation. Other uncertainties are the unspecified injection mechanism for the electrons and their accumulation within the source after cooling (the ``dead electron problem"). In addition, the recent HEXE observations may have ruled out the Zdziarski et al. model in the case of 3C 273 and Cen A. [51]

The (electron) temperature is self-regulated in thermal pair models, due to the combined influence of heating, cooling and pair processes. Haardt and Maraschi [52] considered a coupled two-phase thermal model, in which the cool disk provides the soft photon input for Comptonization in the corona. The hard photons produced contribute to the heating of the cool phase, so that the total spectrum becomes a sum of the power law from the hot phase and the blackbody emission from the disk. Relevant spectra were only obtained when almost all of the energy was dissipated in the hot phase, which the authors argued was due to magnetic reconnection, even though no calculation of magnetic effects was included. Moreover, this model did not include relevant physics associated with pairs (e.g., their stability), as well as with the accretion disk (e.g., transonic flow, advective cooling, multi-temperature structure).

Maraschi and Molendi [53, 54] argued that Comptonization in an optically thin inner disk region should give rise to both the hard X-ray power law and the soft excess. However, the disk model used was of the usual Shakura-Sunyaev type, inappropriate when $\dot{m}$ ~ 1. Furthermore, pair production was neglected even though $T \gtrsim 10^8$ K. One may also note that Comptonization cannot reproduce the observed hard X-ray lag in Cyg X-1. [55]

A hard X-ray power law with a slope (0.5-1.0) is also found in stellar black hole candidates (SBHCs), indicating a production mechanism common to both AGN and SBHC. [56] Obviously, this should then be insensitive to a change in central mass by a factor of ~ 10^8. The slope should also be independent of $\dot{m}$, since an observed flux variation of about three orders of magnitude in GS2000 + 25 had not effect on this parameter. [57]

Next Contents Previous

2.3.3 *X-ray Reflection and Absorption*

Figure 3 shows a single power law fit to the composite spectrum of 12 Ginga observations of 8 Seyferts, whose detailed X-ray properties have been described in Refs. 58-64. The data-minus-model residuals in the lower figure comprise an Fe emission line at 6.4 keV, a dip in the 7-10 keV range and another excess above 12 keV, all of which presumably arise from reprocessing of incident radiation from the central hard X-ray source. The line, which typically has an equivalent width (EW) ~ 150 eV and a breadth (FWHM) ~ a few keV, has been found in $\gtrsim$ 90% of all Seyferts. [65] Figure 4 shows how the EW depends on the incident angle θ, assuming that hard X-rays impinge on a semi-infinite slab of optically thick matter. The solid angle assumed equals 4π, so the expected EW becomes $\delta\omega$ / 4π times smaller, where $\delta\omega$ is the ``real" solid angle. Obviously, observed widths can only be reproduced by a very large θ-value, i.e., the hard X-rays should hit the surface at almost grazing incidence, as in the case of an accretion disk. A spherical geometry cannot produce an EW in excess of ~ 100 eV, and is therefore ruled out. [57] The accretion disk must also be optically thick, in order to produce enough fluorescence flux. [64] The observed correlation between the EW and the relative strength of the soft excess also supports the presence of an accretion disk. [66] Nandra [65] et al. argued that the accretion disk picture seems consistent with available data, in spite of some remaining problems (see below).

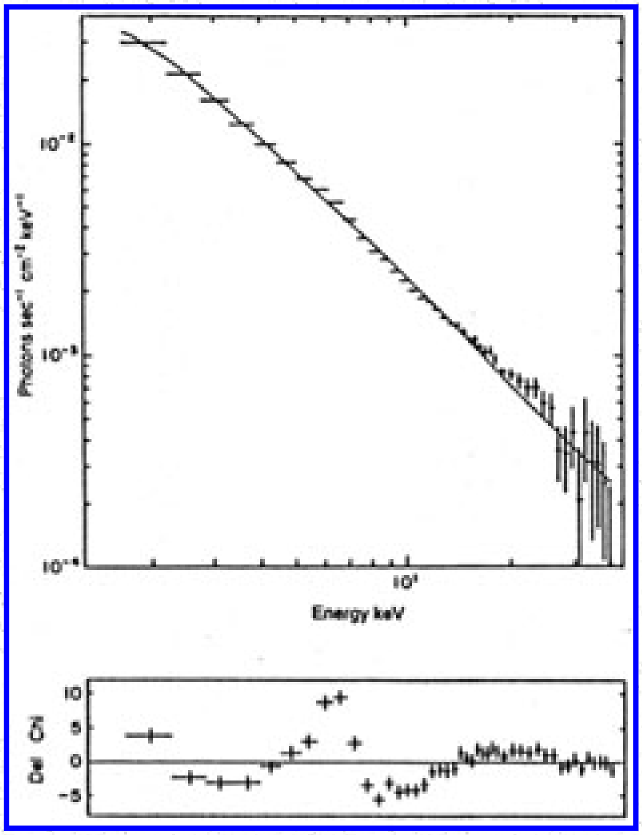

Figure 3. Single power law fit to the composite spectrum of 8 Seyferts, observed by Ginga. A spectral index ~ 0.7 seems to be indicated, but note the residuals in the lower part. An improved model which takes these into account is shown in Fig. 5. From Ref. 57.

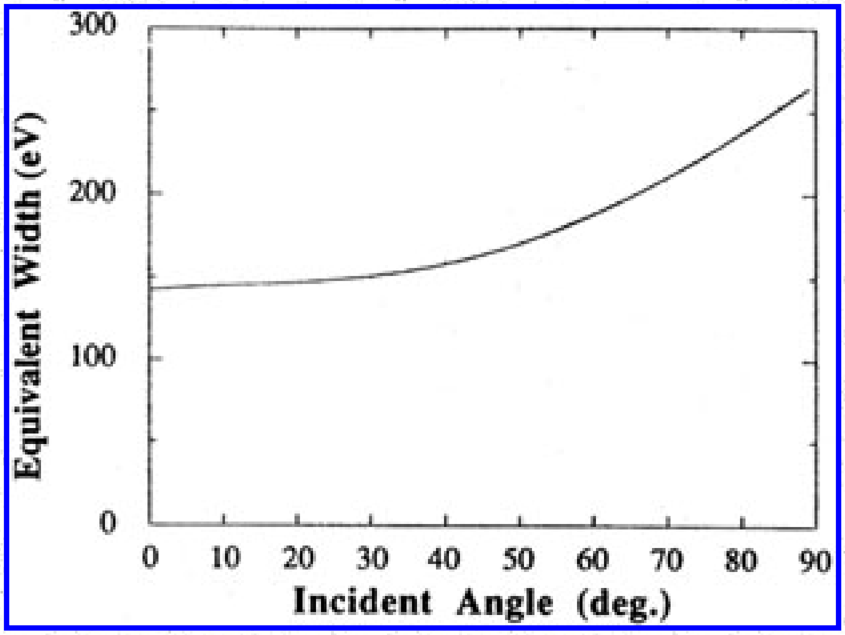

Figure 4. Equivalent widths as a function of incident angle θ, as hard X-rays impinge on a face-on semi-infinite slab of optically thick matter. Observed values can only be reproduced if the hard X-rays are ``reflected" at almost grazing incidence, in support of an accretion disk geometry. From Ref. 57.

The observed FWHM values are consistent [48] with gravitational and Doppler broadening at a typical radius ~ $10r_g$. The 6.4 keV line profile may thus yield important information about physical conditions in the inner disk. A general relativistic formula for the ratio between emitted and observed photon energies, using the Schwarzschild metric, is [67]

$$\frac{\nu_{\rm em}}{\nu_{\rm obs}} = \left(1 - \frac{3r_{\rm g}}{2r_{\rm em}}\right)^{-1/2} \left\{1 + \frac{\cos\beta}{[\varepsilon - 2]^{1/2}}\right\}, \qquad (6)$$

where $\varepsilon = 2r_{em} (1 + \tan^2\zeta) / r_g$, β and ζ being two angles from geometrical optics. Integrating Eq. (6) over the line emitting part of the accretion disk enables a calculation of the line profile. [68] The first term contains the dependence on radius, i.e., the gravitational redshift, whereas the second one yields the kinematic Doppler-shift, which can be either ``blue" or ``red".

Typical profiles obtained using this procedure show some similarities with the double peaked ones in standard theory, but in this case the blue horn appears much brighter than the red one, due to time dilation, aberration and blueshift. A high inclination angle has a similar effect. For low inclination angles *i* the line profile peaks close to its rest energy, but a gravitationally redshifted wing becomes apparent for small radii. The line width increases with *i*, as does the centroid energy. However, Matt et al. [69, 70] have showed that additional features emerge between the two horns for high inclination angles, due to a general relativistic effect. It follows that both the line width and the centroid energy have maxima at about $i \sim 80^{\circ}$.

In principle, X-ray line and continuum variability correlations may be used to map out the core region in AGN, since line-emitting regions close to the central source should be the first to respond to a continuum change. Fabian [48] and Stella [71] argued that the space-time metric and the central mass may then be directly measurable.

Recent observations have cast some doubts on this procedure. [72] The accretion disk should be highly inclined in about 15% of a sample of randomly oriented objects, causing an unobserved centroid redshift $\gtrsim$ 0.2 keV. It is unclear whether this is due to a selection effect, caused by absorption. Furthermore, the large EW (~ 160-300 eV) observed in some sources (such as NGC 6814) seems difficult to explain using the simple models adopted so far. [65]

As regards the other residuals in Fig. 2, the absorption feature at ~ 7-10 keV has been identified with edge absorption, which has also been found in some SBHCs. [57] The excess above 10 keV has been attributed to Comptonized flux which grows with energy, until saturation sets in at a few tens of keV, partly due to incoherence of the scatterings, [31] and partly to the increase of penetrative power, which increases the number of scatterings before the radiation can escape. [73] Figure 5 shows a model which includes the above reflection components (iron K-line and edge), as well as a power law. The spectral index for the ``new'' power law fit is ~ 0.9, somewhat steeper than the standard value.

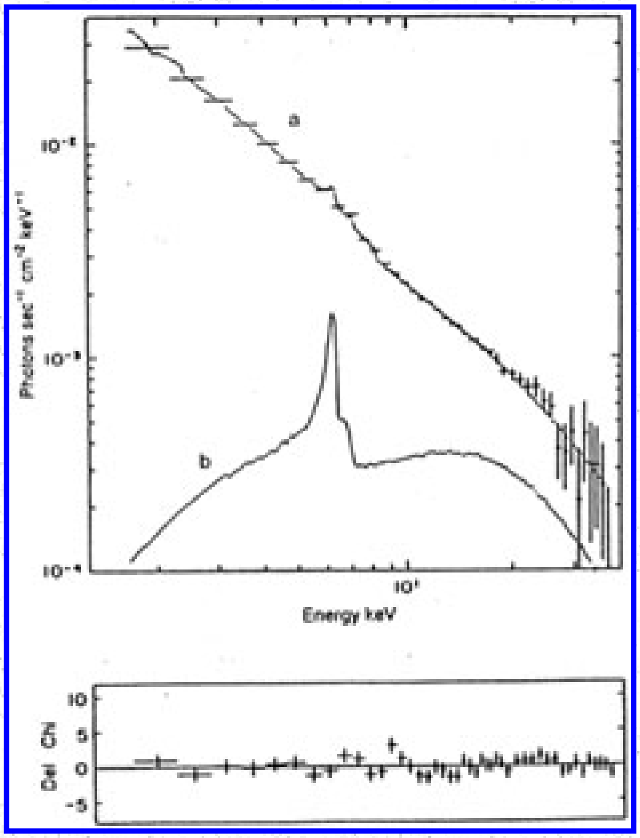

Figure 5. (*a*) Multi-component fit to the same data as in Fig. 3, composed of a power law, the Fe line and edge and a ``warm absorber". (b) Reflection component only. From Ref. 49.

To summarize, it is now established that most Seyfert galaxies indeed show the above X-ray reflection features. The same applies to quasars (QSOs) nearby enough (or bright enough) to yield good-quality X-ray spectra, such as 3C 273 and E1821 + 643. [66, 74, 75] Models which have the ability to include these features will (if successful) have a significant predictive power, but the information content as to the geometry of the reprocessing region, its size and the mass of the central object seems limited at present. However, the fact that X-ray reflection features and a hard X-ray power law with about the same spectral index have been found in both AGN and X-ray binaries may imply that detailed knowledge of the central engine may be gained by comparing different types of objects, using forthcoming X-ray satellites.

2.4 The γ-ray Continuum

Until recently, the only QSO which had been detected in γ-rays was 3C 273. [76] However, the Compton Gamma Ray Observatory has detected about 14 AGN so far, most of which are highly polarized compact radio sources. [77] For instance, the OVV 3C 279 has shown a luminosity [78] ~ 10^{48} (ω / 4π) erg s^{-1} between 100 MeV and 10 GeV, where ω is the solid angle. The apparent superluminal motion in this source should mean that beaming is important. Thus, ω ~ 1 sr yields a γ-ray luminosity ~ 9 x 10^{46} erg s^{-1}, which is still about one order of magnitude higher than the total emission in all other spectral bands. If this also applies to other sources, the dominant radiation from jets may be γ-rays.

It is unclear at present how this radiation is produced. Pelletier [79] has argued that the jet should be composed of electron-positron pairs, whose outflow rate would be ~ 10^{-3} $M_\odot$ yr^{-1}. The Doppler-boost of the luminosity then indicates a Lorentz factor γ ~ 20. Maraschi et al. [80, 81] suggested that the entire IR to γ-ray spectrum of 3C 279 may be explained in terms of an extended version of the inhomogeneous relativistic jet model proposed by Ghisellini et al., [82] and found a Lorentz factor in the range 5-14. They also argued that multiwavelength variability studies may yield information about jets closer to the central engine than feasible with VLBI observations.

Sources with high-energy cutoffs in their γ-ray spectra may be used to constrain pair models. Fabian [33] concluded that the evidence of significant pair production in AGN seems weak at present.

3. THE BROAD-LINE REGION

3.1 Observational Methods

The broad emission lines are quite distinctive features of AGN spectra, and since their generation involves well-understood processes (atomic physics), a wealth of information has been produced, using standard astronomical methods. The basic assumption of current BLR studies is that the line emission is due to photoionization by the continuum. [83] Since the BLR resides well outside the central engine, the observed effects may be regarded as somewhat secondary, being due to reprocessing.

The emission lines can be divided into two varieties: high ionization lines (HIL) such as Lα and CIV λ1550, and low ionization lines (LIL) such as the Balmer and FeII lines. They are normally studied with respect to three different qualities, each with its own method of analysis [84]:

I. Line intensities

These yield information about various physical gas quantities, such as the chemical composition, the electron density and temperature, and the ionization structure. Ratios between various elements are often used. An important fact is that these ratios seem independent of the source luminosity, indicating similar physical conditions (or mechanisms) in both faint and bright objects. Both HIL and LIL are often present simultaneously. About 20 broad (and as many narrow) lines are available for study in a typical AGN.

II. Line profiles

Typical widths of the broad emission lines correspond to gas velocities ~ 1.5 x 10^3-10^4 km s^{-1}. The narrow emission lines are also broad enough to exclude thermal motion. Some profiles are smooth and symmetric, whereas others show clear asymmetries. The latter case may indicate an emission region in radial motion, which is directed inwards if the red wing responds to a continuum change before the blue wing, and outwards in the opposite case. [85] If both wings respond simultaneously, chaotic or circular motion may dominate. [86] Chaotic motion means here that the matter moves along open trajectories in the gravitational field of the central object.

III. Line variability

Spectrophotometric observations have shown that most, perhaps all, Seyfert 1 galaxies have variable broad emission lines. Some QSOs have also shown this behaviour, even though systematic observations are scarce. The line variability usually lags behind the continuum one, in a correlated manner. This constitutes strong evidence in favour of the photoionization hypothesis. The lag is correlated with the luminosity, indicating a more extended BLR in powerful sources.

Next Contents Previous

3.2 The Standard BLR Model

Early photoionization BLR models were quite successful in terms of predicting line ratios in accordance with observed values. [87] After some refinements, a standard model was developed, in which the BLR lines are emitted from cool, dense clouds or filaments, photoionized by the continuum. Clouds are preferred over a continuous matter distribution, since the observed emissivity indicates a ratio ~ 10^{-6} between emitting and total volumes.

One initial suggestion to avoid rapid evaporation of the clouds was a hot ($T \sim 10^8$ K) inter-cloud medium with some unspecified kinematical properties. [88] However, even then the clouds apparently do not last long enough to emit the necessary amount of line radiation. This and other difficulties may have essentially ruled out this scenario. [89] Another suggestion involves magnetic confinement, [90] producing clouds with a filamentary structure along the field lines. The required magnetic field strength would be ~ 1 G, whose origin could lie in a relativistic wind from, e.g., an accretion disk. Still another possibility is a continuous creation of BLR clouds, so that no confinement becomes necessary. Some specific mechanisms for this include (*a*) winds due to mass loss from giant stars, [91] (*b*) orbiting clouds which during infall break up into fragments at about 1 pc from the central source, [92] (*c*) transient shocks [93] and (*d*) thermal instabilities in the inter-cloud medium. [94]

Perhaps the most important parameter in photoionization models is the ionization parameter, one version being defined as

$$U = \frac{Q}{4\pi R^2 N c}, \qquad (7)$$

where Q is the ionizing photon flux, R the distance from the cloud to the continuum source and N the hydrogen number density at the illuminated side of the cloud. Apparently, U measures the degree of ionization in the cloud, dividing the photon flux by the gas density. A specific model for *one* cloud is defined by [89]

- the continuum shape,
- the density or pressure, and the column density,
- the chemical composition,
- the parameter U.

The generalization to *many* clouds involves a pressure and matter distribution over the BLR region. The clouds are assumed to be optically thick, from the presence of strong MgII and FeII lines. Broad forbidden lines are often absent, indicating a typical cloud density ~ 10^8-10^{10} cm^{-3}. Chemical abundances are assumed to lie around the solar value (within a factor of 3). Using these values and $U \sim 10^{-2}$, the BLR size as deduced from Eq. (7) becomes ~ 0.1 and ~ 2 pc for Seyferts and bright QSOs, respectively.

The standard BLR model has recently encountered an increasing number of difficulties. Thus, the high ionization lines (such as NV λ1240) are stronger than predicted and the strong FeII lines in some objects are difficult to explain, and the correlation between obtained results (e.g., line ratios) and the shape of the continuum is rather small. [95] The attempts to use photoionization codes for revealing accretion disks as the continuum source therefore seem futile. [96] Furthermore, the standard *U*-value is significantly exceeded in some sources. [97] Finally, the NGC 5548 campaigns may have ruled out the customary one-zone type of model.

3.3 Recent Developments

3.3.1 *The NGG 5548 and 4151 Campaigns*

The aim of the NGC 5548 campaigns (using IUE and ground-based optical observations) was to monitor the variability with an unprecedented sampling rate, in both the continuum and the lines. A previous and similar study was devoted to NGC 4151, from which Ulrich et al. [98] concluded that the continuum variability in UV and optical was simultaneous, with an upper time limit for the delay $\lesssim$ 2 days. The timescale of the variability was also of this order, which may have ruled out an origin due to local thermal disk instabilities. There was also a significant correlation between variations in UV-optical and X-rays on at least one occasion. Some of the NGC 5548 results [99]-[101] can be summarized as follows:

I. Ionization structure

The delay between continuum and line variations was smaller for highly ionized elements, and the line variability amplitude increased with the degree of ionization. This reinforces the belief in the photoionization hypothesis, and shows that the BLR is stratified.

II. Geometry

Krolik [19], [102] and collaborators argued that detailed model-fitting implies that the HIL are emitted from a spherical region, whereas the LIL should be emitted from a flattened geometry, such as an accretion disk. That the HIL and LIL do not arise in the same region is indicated by their different profiles and redshifts. [103] The customary one-zone BLR model is thus not applicable.

III. Dynamics

Gaskell [85] used the cross-correlation technique on the wings of the CIV line in NGC 4151, and argued that radial inflow of the BLR clouds was indicated. The same arguments were applied to Fairall 9 (F9) [104] and NGC 5548. [105] In contrast, Clavel et al. [99] found no evidence of radical motion in the latter source, and argued in favour of chaotic or rotational motion. According to Ulrich, [72] the fast moving clouds should not cross the accretion disk, as in the case of chaotic motion. The clouds emitting the HIL should then remain on the same side of the disk after formation, and other forces (e.g., radiative or magnetic) besides gravitation may influence the cloud motion. The temporal behaviour of the CIV line wings in NGC 4151 also indicates that the spatial distribution of the clouds changes on a timescale ~ years, which may signal the arrival of new material from the inner BLR. [98]

IV. Size

The CIV line is frequently used in BLR size estimates. The peak value of the cross-correlation between this line and the continuum is ~ 8 days, whereas the centroid amounts to ~ 31 days, which approximately correspond to the inner BLR radius and an ``average", luminosity-weighted one, respectively. [106] Both of these values are consistent with those found in the campaigns, and the inferred BLR size (~ 0.01 pc) is about *one order of magnitude* lower than the standard value. Moreover, the stratification implies a distribution of clouds with different sizes, temperatures and distances from the continuum source. The concept of a single BLR ``radius" may thus be replaced by a range, amounting to 10-100 light-days. [97] A size smaller than the standard value has also been found in F9, Mrk 279, NGC 4151 and Akn 120. [89]

Next Contents Previous

3.3.2 *The Accretion Disk Model*

The standard Shakura-Sunyaev disk model is difficult to reconcile with the almost simultaneous variability in UV, optical and X-rays in NGC 4151 and NGC 5541, indicating that illumination by the hard X-ray source may give rise to a large fraction of the UV-optical flux through reprocessing. [99, 107] However, it could be that these sources are atypical examples, as pointed out before. Indeed, there seems to be no correlation between variations in UV-optical and X-rays in most AGN. Ulrich et al. [98] suggested instead that the varying part of the optical flux is the low-energy tail of the UV-bump, thereby producing simultaneous UV-optical variability. They also argued that the latter may be due to disk instabilities in the inner region.

However, one advantage of the illumination model is that the LIL may be explained this way. Collin-Souffrin and collaborators (e.g., Ref. 108) have developed such a model, whose basic assumption is an extended accretion disk (to at least $R \sim 10^4 r_g$). One problem with the model has been the condition of negligible self-gravity, which imposes an upper limit on $\dot{m}$. In F9 this would translate into a highly supersonic turbulence, which seems unphysical. A recent version [32, 103] avoided this problem by adopting a small $\dot{m}$-value. The LIL emission region was confined to $R \sim 10^2$-$10^4 r_g$, since line saturation for $R \lesssim 10^2 r_g$ and inadequate heating for $R \gtrsim 10^4 r_g$ inhibit line formation in other regions. The result seems able to meet quite a number of observational constraints. Thus, the line widths may be explained in terms of kinematics, since $v_K(10^3 r_g) \sim 10^3$ km s^{-1}, where v_K is the Keplerian rotational velocity. The large column density and covering factor required to explain the intensity of the LIL and the formation and confinement problems may also be accounted for. Furthermore, the constancy of line ratios may be explained by quasi-thermalization of the lines.

The model requires that a sizeable fraction (~ 1/2) of the bolometric luminosity is emitted in hard X-rays or γ-rays. The bulk of the UV luminosity should then be emitted by the accretion disk, of which a part is due to reprocessing. By combining the fitting procedures for the UV continuum and line emission from the disk, the obtained accretion rate was much lower than the one estimated from the bolometric luminosity. One explanation may be that the ``real" accretion rate is higher, but that only part of the liberated gravitational energy comes out in optical-UV. The rest may be dissipated in a hot, optically thin phase. as in the Haardt and Maraschi model discussed above.

The applicability of these results to other AGN such as OSOs remains an open issue. Even though rapid broad line variability has been detected in QSOs, the under-sampling usually precludes definite conclusions. The BLR lines also seem to respond to a continuum change in a very complicated fashion. Furthermore, some sources show rapid continuum variability, but no line variability. Such null-results may yield interesting constraints on, e.g., the BLR geometry.

To summarize, a picture of a much smaller BLR and brighter continuum source than previously thought has emerged. The most promising method to map out the BLR may involve further developments of the cross-correlation technique, such as the echo mapping (1D, 2D or 1D + time) proposed by Welsh and Horne [109] and further discussed by Horne.[110] The number of unsettled issues is still large, some of which include:

- how are the clouds formed and destroyed?
- if confinement is required, how is that achieved?
- what determines the kinematics, and what motion dominates the velocity field?
- is the overall geometry spherical (as in the standard model), or flattened (as in the accretion disk model), or a combination of both?
- how is the intermediate torus related to the narrow-line region (NLR), the BLR and the accretion disk?
- are jets and the BLR clouds somehow connected?

Next Contents Previous

4. THE CENTRAL BLACK HOLES IN ACTIVE GALACTIC NUCLEI

4.1 Formation

Obviously, the formation of central black holes in AGN should be closely connected with the issues of galaxy formation and evolution. The onset of AGN activity may be delayed with respect to galaxy formation, since a deep enough potential well is required. [111] The duration of the lag depends on the precursor history, ranging from ~ 10^9 years in the case of a relativistic cluster of stellar compact objects [112] to about ~ $10 M_8^{-1}$ years for a supermassive radiation pressure supported star, radiating at the Eddington limit. [113]

The complexities of the black hole formation process must in general be investigated numerically. The outcome depends on a variety of factors, including the amount of rotation, the fuel supply, the gas and dust distribution, the stellar density and velocity dispersion (which determine the collision rate), and so on. It seems more likely that the early evolution leads to a single stellar black hole, surrounded by predominantly normal stars and gas, rather than to the relativistic cluster of ~ 10^8 compact objects within a volume ~ 10 r_g across, assumed as an initial condition by Shapiro and Teukolsky. [112] Ozernoy[114] found (analytically) that central black holes of various sizes were obtainable, provided the initial velocity dispersion and core density were high enough. Other numerical simulations showed that the evolution from a single seed black hole of a mass M ~ 10^3 $M_\odot$ should lead to a supermassive one. These simulations usually offer no explanation as to the origin of such a seed hole. However, Quinlan and Shapiro [115] showed that formation may arise rather easily from stellar mergers in a dense, but otherwise normal galactic nucleus.

4.2 Methods of Inferring the Mass

As pointed out by Richstone, [116] one possibility to infer the presence of black holes is first to determine the central mass, and then to rule out alternatives to a black hole. This is similar to the stellar case within our Galaxy, where the central mass in some cases exceeds the maximal one allowed for a neutron star. [117] Methods of inferring the central mass in AGN include:

I. Stellar kinematics

The black hole hypothesis implies the existence of central black holes in nearly all galaxies. Interestingly, recent observations have indicated the presence of dark, massive concentrations of matter in nearby galactic nuclei. The basis of these investigations is the collisionless Boltzmann equation

$$M = \frac{v^2 R}{G} + F(\rho, R, \sigma_r, \sigma_\theta, \sigma_\phi), \qquad (8)$$

where v is a typical rotation velocity, R the size scale, F a function of the deprojected star density ρ and the three deprojected components of the velocity dispersion σ_r, σ_θ and σ_ϕ. Using various kinematic stellar models to fit the data, the result is $M_8 \sim 0.1$ for M31 [118] and ~ 0.6 for M32, [116, 119] ~ 10 for NGC 4594 [120] and ~ 1-10 for NGC 3115. [121, 122] The famous case of M87 seems unsettled at present. [123]

It should be stressed that even though this approach may have given support to the first of Richstone's steps, the second one still remains to be done. Indeed, the central mass can, for instance, comprise a non-relativistic, compact cluster of low-mass stars, instead of a black hole. [116] The observed stellar motion could also be influenced by forces from outside the galactic nucleus, and the inherent assumptions of the stellar kinematical models may be irrelevant. Furthermore, the method seems limited to nearby, edge-on and fast rotating spiral galaxies. [122]

II. Bolometric luminosity

The basic accretion formula $L = \varepsilon \dot{M} c^2$ yields

$$M \sim \frac{LT}{\varepsilon c^2}, \qquad (9)$$

where T is the lifetime of the AGN. If we assume (from, e.g., the extension of extragalactic jets) $T \sim 10^8$ years, a luminosity ~ 10^{46} ergs s^{-1} and $\varepsilon \sim 0.1$, we obtain $M_8 \sim 0.1$. In practice, only L is an observable, so statistical arguments (involving radiation density estimates from QSO counts) are invoked. [117, 117] The result lies in the range M_8 ~ 0.1-10. The nature of individual central objects may be difficult to determine using this method.

III. Properties of the broad-line region

The basic assumption is that the cloud motion is purely gravitational, which, as discussed above, may be irrelevant. The first term in Eq. (8) is used, where now *v* is the BLR cloud velocity and R the BLR size. In addition, a multiplying factor γ ~ 1 is usually added, whose value depends on whether the motion is bound or not. Gaskell [85] pointed out that the *direction* of the motion is also needed, since a pure outflow says very little about the central mass. Some results for nearby Seyferts are: M_8 ~ 0.1 for NGC 5548, [105] ~ 0.5 for NGC 4151 [85] and ~ 8 for F9. [104] In order to establish the necessary infall of matter, the method uses the cross-correlation technique between line wing variations. The uncertain size and velocity field structure discussed above limit the relevance of this method. Also, the nature of the central object seems difficult to infer, since the BLR effects occur outside the central engine.

IV. Continuum properties

Accretion disk spectra have been rather successfully fitted to UV-optical continua. [27, 36] The original models have been extended to include general relativistic, geometrical and opacity effects. Since the central engine is utilized, the reliability of the method may be higher than for previous approaches.

A higher inclination angle implies a harder spectrum, whereas a higher mass has the opposite effect (the maximum disk temperature is inversely proportional to the mass). The result is a correlation between the inclination angle and the mass, which reduces the number of fitting parameters from three to two: [$\dot{M}$, *M*(cos *i*)]. Although these two parameters can be constrained rather tightly, the allowed range in central mass becomes large, since the inclination angle is undetermined. Typical results for a disk without reprocessing are M_8 ~ 0.1-10 for Seyfert 1s and M_8 ~ 1-100 for elliptical galaxies. [36]

The cases which show simultaneous variability in UV and optical probably require that reprocessing must also be taken into account. Malkan [126] adopted a simple model, in which reprocessing was assumed to dominate outside a critical disk radius r_c, whereas the emission was due to ``normal'' viscous dissipation inside $r_c$. Moving the latter inwards obviously increases the relative fraction of reprocessed optical flux, amounting to ~ 27% for $r_c$ ~ 25 $r_g$. Since the reprocessed flux comes out in optical and UV, the ``original'' disk emission in these ranges must be decreased, which is accomplished by a decrease in the central mass. In the case of NGC 5548, consistency requires M_8 to decrease from 2 to 0.55. This in turn implies a hotter disk, which shifts much of the emission into the unobserved EUV region.

If problems concerning the adopted disk model (usually of the inappropriate Shakura-Sunyaev type), the inclination angle, the reprocessing and relative contributions from stars and the BLR can be resolved, spectral fits using accretion disks may provide reliable estimates of the central mass.

V. X-ray variability - NGC 6814

The short (~ 10^3 s) variability timescale in X-rays indicates an origin also in the central engine (cf. Eq. (2)). The only AGN which so far has shown clear evidence of quasi-periodic X-ray variability is NGC 6814. [127, 128] The peaks in the power spectrum lie in the range $10^{-4\pm1}$ Hz, and the variability period (~ 10^4 s) has been shown to be rather constant over timescales of years, indicating [129] $|\dot{P}| \lesssim 10^{-6}$. The period also seems virtually uncoupled to luminosity (and hence accretion rate) variations.

There are essentially four classes [130] of proposed explanations for the variability of NGC 6814, of which the first three involve a single spot orbiting on the accretion disk surface, [131, 132] collisions between a star and the accretion disk [133-135] and an orbiting screen in the outer disk. [136, 137] All of these may suffer from being fine tuned, and the reason why the screen should have an approximately stable structure seems obscure. The spot and screen models may have encountered further difficulties due to the change of folded light-curve structure between the EXOSAT and Ginga observations. This change may be explained by Lense-Thirring precession of the orbit of the star in the collisional model, [133] but the indication of $\dot{P} > 0$ may have imposed major difficulties for this scenario, since the opposite effect is expected. [138]

The fourth alternative makes use of acoustic mode behaviour in the innermost part of the accretion disk. [10] The slim disk acoustic instability frequency increases generally with $\dot{m}$, which partially may explain the horizontal branch oscillations (HBOs) observed in X-ray binaries. [9] However, the instability frequency becomes essentially constant (for a specific radius), when the accretion rate is low (Fig. 6). Thus, the only model which at present seems able to explain the stability and the numerical value of the period, its long-term trend (as indicated by $\dot{P} > 0$) as well as the change of topology of the folded light-curve may be the acoustic one. [139] Also, the presence of a supermassive black hole in NGC 6814 seems strongly supported, since a central mass $M_8 \sim 10^{-2}$ then would reside within a volume only a few Schwarzschild radii across. Independent global, numerical and time-dependent calculations of acoustic mode behaviour [140, 141] are consistent with this conclusion. Provided the acoustic model holds true, the same behaviour should also apply to other sources, if the inner accretion disk can be observed, and if the accretion rate is low. A search for such sources should consequently concentrate on nearby, low-luminosity and face-on AGN, or their stellar galactic counterparts.

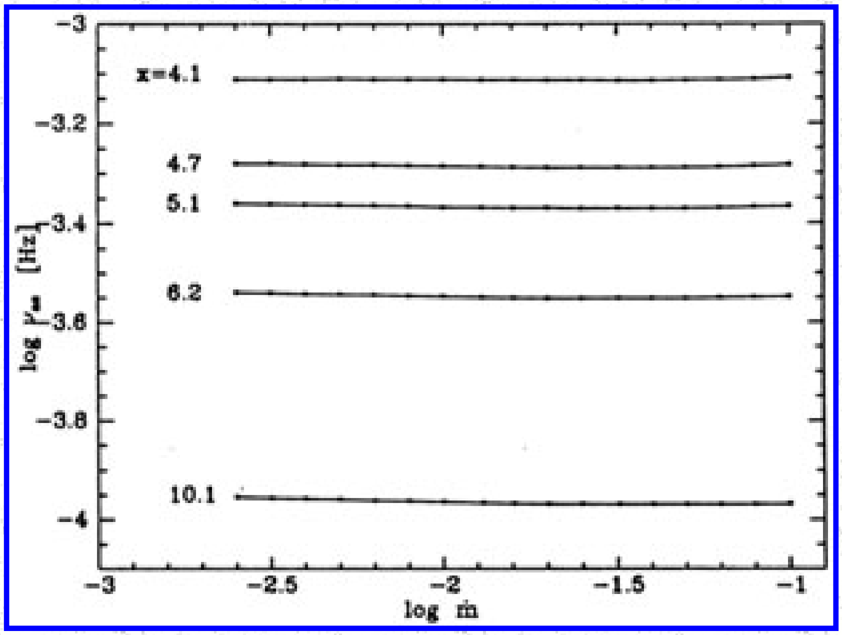

Figure 6. The relation between acoustic instability frequency ν_{ac} and accretion rate $\dot{m}$ in the inner region of a slim disk. The quantity *x* is the radius in Schwarzschild units. From Ref. 139.

Next Contents Previous

5. CONCLUSIONS

Even though one may easily stress our ignorance of how the central engine in AGN operates, some observational and theoretical progress has probably already been made. Reprocessing seems to be significant. perhaps giving rise to the low-ionization lines and partly to the IR, optical-UV and X-ray continua. The X-ray reflection features provide evidence of cold, optically thick matter, and are consistent with a flattened geometry, such as an accretion disk. It remains to be seen how the BLR, the NLR and the intermediate torus and possibly the jets are related to the central accretion disk. The customary Shakura-Sunyaev approach seems inadequate in this exploration process, since several effects are not included. However, the more relevant slim disks will probably also require modification, since the soft X-ray excess and the hard X-ray power law seem difficult to reproduce. One solution could be to include a hot, optically thin plasma in or near the inner disk. A significant part of the liberated gravitational energy may then be dissipated in this region, thereby producing the hard X-rays which subsequently get reprocessed into lower-energy radiation in several steps. Both the geometry of and the dominant physical processes in the hot phase are unsettled, but may involve Comptonization, pair production or magnetic fields in a corona or disk annulus.

As a first step towards physical understanding of AGN, the existence of both accretion disks and black holes needs to be settled. If a method of estimating the central mass is to be reliable, alternatives which involve the central engine may be more appropriate. Due to the inherent problems with UV-continuum fits, essentially two possibilities remain: interpretation of X-ray continuum variability or of Fe fluorescence line profile variations. Since the latter alternative awaits adequate spectral resolution, the best current evidence of black holes in AGN seems to come from variability studies, as exemplified by NGC 6814.

The striking similarities between spectral features (blue bump, X-ray reflection features, hard X-ray power law, quasi-periodic variability and so on) observed in AGN and X-ray binaries may indicate the need for a general model, applicable to both stellar and extra-galactic systems. If combined with the results from forthcoming X-ray satellites (such as XMM and AXAF), such a model should be able to constrain or even deduce physical conditions in compact sources.

Acknowledgments

Prof. M. Abramowicz, Prof. B. Pagel and Prof. R. Svensson are thanked for their comments on the manuscript. Financial support from the Royal Swedish Academy of Sciences, the Royal Physiographical Society of Lund and the Swedish Natural Science Research Council is gratefully acknowledged.

F.H. WALLINDER
NORDITA,

Blegdamsvej 17,
DK-2100 Copenhagen Ø, Denmark

Contents Previous

REFERENCES

1. M.C. Begelman, R. D. Blandford and M. J. Rees, Rev. Mod. Phys. **56**, 255 (1984).
2. M.J. Rees, Ann. Rev. Astron. Astrophys. **22**, 471 (1984).
3. N.I. Shakura and R.A. Sunyaev, Astron. Astrophys. **24**, 337 (1973).
4. N.I. Shakura and R.A. Sunyaev, Mon. Not. R. Astr. Soc. **175**, 613 (1976).
5. M.A. Abramowicz, M.A. Malkan and E. Szuszkiewicz (1992, in preparation).
6. T.J.L. Courvoisier and J. Clavel, Astron. Astrophys. **248**, 389 (1991).
7. M.A. Abramowicz, B. Czerny. J.-P. Lasota and E. Szuszkiewicz, Astrophys. J. **332**, 646 (1988).
8. M.A. Abramowicz, F. Szuszkiewicz and F. Wallinder, *Theory of Accretion Disks*, eds. F. Meyer, W.J. Duschl, J. Frank and E. Meyer-Hofmeister, NATO ASI Series Vol. 290 (Kluwer, 1989), p. 141.
9. F.H. Wallinder, Astron. Astrophys. **249**, 107 (1991).
10. F.H. Wallinder, Mon. Not. R. Astr. Soc. **253**, 184 (1991).
11. M.C. Begelman, *Accretion Disks and Magnetic Fields in Astrophysics*. eds. G. Belvedere et al. (Kluwer, 1989), p. 255.
12. R. Barvainis, Astrophys. J. **353**, 419 (1990).
13. T. Nakajima, N.P. Carleton and M. Nishida, Astrophys. J. **375**, L1 (1991).
14. G. Berriman, Astrophys. J. **354**, 148 (1990).
15. A.S. Wilson, *Physics of Active Galactic Nuclei*, eds. W.J. Duschl and S.J. Wagner (Springer-Verlag, 1992), p. 307.
16. T. Storchi-Bergmann, J.S. Mulchaey and A.S. Wilson, Astrophys. J. **395**, 73 (1992).
17. P. Madau, Astrophys. J. **327**, 116 (1988).
18. R.R.J. Antonucci and J.S. Miller, Astrophys. J. **297**, 621 (1985).
19. J.H. Krolik, *Testing the AGN Paradigm*, eds. S.S. Holt, S.G. Neff and C.M. Urry, AIP Conf. No. 254 (1992), p. 473.
20. J.N. Bregman, Astron. Astrophys. Rev. **2**, 125 (1990).
21. C.M. Urry, L. Maraschi and E.S. Phinney, Comments Astrophys. **15**, 111 (1991).
22. S. Djorgovski, N. Weir, K. Matthews and J.R. Graham, Astrophys. J. **372**, L67 (1991).
23. M.J. Ward, P.R. Blanco, A.S. Wilson and M. Nishida, Astrophys. J. 382, 115 (1991).
24. E.S. Phinney, *Theory of Accretion Disks*, eds. F. Meyer, W.J. Duschl, J. Frank and E. Meyer-Hofmeister, NATO ASI Series Vol. 290 (Kluwer, 1989), p. 457.
25. G.A. Shields, Nature **272**, 706 (1978).
26. M.A. Malkan and W.L.W. Sargent, Astrophys. J. **254**, 22 (1982).
27. M.A. Malkan, Astrophys. J. **268**, 582 (1983).
28. J. Clavel, K. Nandra, F. Makino, K.A. Pounds, G.A. Reichert, C. M. Urry, W. Wamsteker, M. Peracaula-Bosch, G.C. Stewart and C. Otani, Astrophys. J. **393**, 113 (1992).

29. M.A. Malkan (1992, personal communication).
30. P.W. Guilbert and M.J. Rees, Mon. Not. R. Astr. Soc. **233**, 475 (1988).
31. A.P. Lightman and T.R. White, Astrophys. J. **335**, 57 (1988).
32. S. Collin-Souffrin, *Testing the AGN Paradigm*, eds. S. . Holt, S.G. Neff and C.M. Urry, AIP Conf. No. 254 (1992), p. 119.
33. A.C. Fabian, *Testing the AGN Paradigm*, eds. S.S. Holt, S.G. Neff and C.M. Urry, AIP Conf. No. 254 (1992), p. 657.
34. E.M. Puchnarewicz, K.O. Mason, F.A. Cordova, J. Kartje, G. Branduardi-Raymont, J.P.D. Mittaz, P.G. Murdin and J. Allington-Smith, Mon. Not. R. Astr. Soc. **256**, 589 (1992).
35. T.J. Turner and K.A. Pounds, Mon. Not. R. Astr. Soc. **240**, 833 (1989).
36. W.H. Sun and M.A. Malkan, Astrophys. J. **346**, 68 (1989).
37. B. Czerny and M. Elvis, Astrophys. J. **321**, 305 (1987).
38. M.H. Ulrich, *Theory of Accretion Disks*, eds. F. Meyer, W.J. Duschl, J. Frank and E. Meyer-Hofmeister, NATO ASI Series Vol. 290 (Kluwer, 1989), p. 3.
39. J.S. Kaastra and P. Barr, Astron. Astrophys. **226**, 59 (1989).
40. K.A. Pounds and I.M. McHardy, *Physics of Neutron Stars and Black Holes*, ed. Y. Tanaka (Universal Academic Press, Tokyo, 1988).
41. A.A. Zdziarski and P.S. Coppi, Astrophys. J. **376**, 480 (1991).
42. R.F. Mushotzky, Adv. Sp. Res. **3**, 10 (1984).
43. A.A. Zdziarski and A.P. Lightman, Astrophys. J. **294**, L79 (1985).
44. A.C. Fabian, R.D. Blandford, P.W. Guilbert, E.S. Phinney and L. Cuellar, Mon. Not. R. Astr. Soc. **221**, 931 (1986).
45. R. Svensson, Mon. Not. R. Astr. Soc. **227**, 403 (1987).
46. C. Done, G. Ghisellini and A.C. Fabian, Mon. Not. R. Astr. Soc. **245**, 1 (1990).
47. C. Done and A.C. Fabian, Mon. Not. R. Astr. Soc. **240**, 81 (1989).
48. A.C. Fabian, *ESLAB Symp. on Two Topics in X-Ray Astronomy* (ESA SP-296, 1989), p. 1097.
49. K.A. Pounds, K. Nandra, G.C. Stewart, I.M. George and A.C. Fabian, Nature **344**, 132 (1990).
50. A.A. Zdziarski, G. Ghisellini, I.M. George, R. Svensson, A.C. Fabian and C. Done, Astrophys. J. **363**, L1 (1990).
51. M. Maisack et al., Astron. Astrophys. **262**, 433 (1992).
52. F. Haardt and L. Maraschi, Astrophys. J. **380**, L51 (1991).
53. L. Maraschi and S. Molendi, *ESLAB Symp. on Two Topics in X-Ray Astronomy* (ESA SP-296, 1989), p. 981.
54. L. Maraschi and S. Molendi, Astrophys. J. **353**, 452 (1990).
55. S. Miyamoto, S. Kitamoto, M. Kazuhisa and T. Dotani, Nature **336**, 450 (1988).
56. Y. Tanaka, ESLAB Symp. on Two Topics in X-Ray Astronomy (ESA SP-296, 1989), p. 3.
57. H. Inoue, *ESLAB Symp. on Two Topics in X-Ray Astronomy* (ESA SP-296, 1989), p. 783.
58. K.A. Pounds, V.J. Stanger, T.J. Turner, A.R. King and B. Czerny, Mon. Not. R. Astr. Soc. **224**, 443 (1987).
59. T.J. Turner and K.A. Pounds, Mon. Not. R. Astr. Soc. **232**, 463 (1988).

60. K. Nandra, K.A. Pounds, G.C. Stewart, I.M. George and A.C. Fabian, *ESLAB Symp. on Two Topics in X-Ray Astronomy* (ESA SP-296, 1989), p. 1021.
61. K. Nandra, K.A. Pounds and G.C. Stewart, Mon. Not. R. Astr. Soc. **242**, 660 (1990).
62. K.A. Pounds, *ESLAB Symp. on Two Topics in X-Ray Astronomy* (ESA SP-296, 1989), p. 753.
63. L. Piro, M. Matsuoka and M. Yamauchi, *ESLAB Symp. on Two Topics in X-Ray Astronomy* (ESA SP-296, 1989), p. 819.
64. I.M. George, K. Nandra and A.C. Fabian, Mon. Not. R. Astr. Soc. **242**, 28 (1990).
65. K. Nandra, K.A. Pounds and G.C. Stewart, *Testing the AGN Paradigm*, eds. S.S. Holt, S.G. Neff and C.M. Urry, AIP Conf. No. 254 (1992), p. 163.
66. M.J.L. Turner, O.R. Williams, R. Saxton, G.C. Stewart, T.J.L. Courvoisier, T. Ohashi, K. Makishima, T. Kii and H. Inoue, *ESLAB Symp. on Two Topics in X-Ray Astronomy* (ESA SP-296, 1989), p. 769.
67. L. Stella and S. Campana, *Iron Line Diagnostics in X-ray Sources*, eds. A. Treves, G.C. Perola and L. Stella (Springer-Verlag, 1991), p. 230.
68. A.C. Fabian, M.J. Rees, L. Stella and N.E. White, Mon. Not. R. Astr. Soc. **238**, 729 (1989).
69. G. Matt, G.C. Perola, L. Piro and L. Stella, Astron. Astrophys. **257**, 63 (1992).
70. G. Matt, G.C. Perola, L. Piro and L. Stella, Astron. Astrophys. **263**, 453 (1992).
71. L. Stella, Nature **344**, 747 (1990).
72. M.H. Ulrich, *Testing the AGN Paradigm*, eds. S.S. Holt, S.G. Neff and C.M Urry, AIP Conf. No. 254 (1992), p. 539.
73. T.R. White, A.P. Lightman and A.A. Zdziarski, Astrophys. J. **331**, 939 (1988).
74. M.J.L. Turner, O. R. Williams, T.J.L. Courvoisier, G.C. Stewart, K. Nandra, K.A. Pounds, T. Ohashi, K. Makishima, H. Inoue, T. Kii, F. Makino, K. Hayashida, Y. Tanaka, S. Takano and K. Koyama, Mon. Not. R. Astr. Soc. **244**, 310 (1990).
75. T. Kii, O.R. Williams, T. Ohashi, H. Awaki, K. Hayashida, H. Inone, H. Kondo, K. Koyama, F. Makino, K. Makishima, R.D. Saxton, G.C. Stewart, S. Takano, Y. Tanaka and M.J.L. Turner, Astrophys. J. **367**, 455 (1991).
76. G.F. Bignami et al., Astron. Astrophys. **93**, 71 (1981).
77. C.D. Impey, *The Nature of Compact Objects in AGN* (Cambridge University Press, in preparation).
78. R.C. Hartman et al., Astrophys. J. **385**, L1 (1992).
79. G. Pelletier (1992, personal communication).
80. L. Maraschi, G. Ghisellini and A. Celotti, *Testing the AGN Paradigm*, eds. S.S. Holt, S.G. Neff and C.M. Urry, AIP Conf. No. 254 (1992), p. 439.
81. L. Maraschi, G. Ghisellini and A. Celotti, preprint.
82. G. Ghisellini, L. Maraschi and A. Treves, Astron. Astrophys. **146**, 204 (1985).
83. J.H. Krolik, *Active Galactic Nuclei*, eds. R.H. Miller and P.J. Wiita (Springer-Verlag, 1988), p. 19.
84. H. Netzer, *Active Galactic Nuclei*, eds. T.J.L. Courvoisier and M. Mayor (Springer-Verlag, 1990), p. 57.
85. C.M. Gaskell, Astrophys. J. **325**, 114 (1988).

86. R.D. Blandford and C.F. McGee, Astrophys. J. **255**, 419 (1982).
87. K. Davidson, Astrophys. J. **171**, 213 (1972).
88. J.H. Krolik, C.F. McGee and C.B. Tarter, Astrophys. J. **249**, 422 (1981).
89. H. Netzer, Comments Astrophys. **14**, 137 (1989).
90. M.J. Rees, Mon. Not. R. Astr. Soc. **228**, 47 (1987).
91. D. Kazanas, Astrophys. J. **347**, 74 (1989).
92. T.J. Carroll, Mon. Not. R. Astr. Soc. **214**, 321 (1985).
93. J.J. Perry and J.E. Dyson, Mon. Not. R. Astr. Soc. **213**, 665 (1985).
94. J.H. Krolik, Astrophys. J. **325**, 148 (1988).
95. A. Binette, A. Robinson and T.J.L. Courvoisier, Astron. Astrophys. **194**, 65 (1988).
96. J.H. Krolik and T.R. Kallman, Astrophys. J. **324**, 714 (1988).
97. A.P. Koratkar (1992, personal communication).
98. M.H. Ulrich, A. Boksenberg, G.E. Bromage, J. Clavel, A. Elvius, M. V. Penston, G.C. Perola and M.A.J. Snijders, Astrophys. J. **382**, 483 (1991).
99. J. Clavel et al., Astrophys. J. **366**, 64 (1991).
100. B.M. Peterson et al., Astrophys. J. **368**, 119 (1991).
101. B.M. Peterson et al., Astrophys. J. **392**, 470 (1992).
102. J.H. Krolik, K. Horne, T.R. Kallman, M.A. Malkan, R.A. Edelson and G.A. Kriss, Astrophys. J. **371**, 541 (1991).
103. E. Rokaki, C. Boisson and S. Collin-Souffrin, Astron. Astrophys. **253**, 57 (1992).
104. A.P. Koratkar and C.M. Gaskell, Astrophys. J. **345**, 637 (1989).
105. D.M. Crenshaw and J.H. Blackwell, Astrophys. J. **358**, L37 (1990).
106. A.P. Koratkar and C.M. Gaskell, Astrophys. J. **375**, 85 (1991).
107. J. Clavel, *Variability of Active Galactic Nuclei*, eds. H.R. Miller and P.J. Wiita (Cambridge University Press, 1991), p. 301.
108. S. Collin-Souffrin and A.M. Dumont, Astron. Astrophys. **229**, 292 (1990).
109. W.F. Welsh and K. Horne, Astrophys. J. **379**, 586 (1991).
110. K. Horne, *The Nature of Compact Objects in AGN* (Cambridge University Press, in preparation).
111. M.J. Rees, *Structure and Evolution of Active Galactic Nuclei*, eds. G. Giuricin et al. (Reidel, 1986), p. 447.
112. S.L. Shapiro and S.A. Teukolsky, Astrophys. J. **298**, 34 (1985).
113. S.L. Shapiro and S.A. Teukolsky, *Black Holes, White Dwarfs and Neutron Stars - The Physics of Compact Objects* (Wiley, 1983).
114. L. Ozernoy, *Supermassive Black Holes*, ed. M. Kafatos (Cambridge University Press, 1988), p. 211.
115. G.D. Quinlan and S.L. Shapiro, Astrophys. J. **356**, 483 (1990).
116. D.O. Richstone, *Supermassive Black Holes*, ed. M. Kafatos (Cambridge University Press, 1988), p. 87.
117. J. McClintock, Adv. Sp. Res. **8**, 367 (1988).
118. J. Kormendy, *Supermassive Black Holes*, ed. M. Kafatos (Cambridge University Press, 1988), p.

98.
119. A. Dressler and D.O. Richstone, Astrophys. J. **324**, 701 (1988).
120. J. Kormendy, Astrophys. J. **335**, 40 (1988).
121. J. Kormendy and D. Richstone, Astrophys. J. **393**, 559 (1992).
122. J. Kormendy, *Testing the AGN Paradigm*, eds. S.S. Holt, S.G. Neff and C.M. Urry, AIP Conf. No. 254 (1992), p. 23.
123. A. Dressler, *Active Galactic Nuclei*, eds. D.E. Osterbrock and J. S. Miller (IAU Symp. No. 134, 1989), p. 217.
124. A. Soltan, Mon. Not. R. Astr. Soc. **200**, 115 (1982).
125. A. Chokshi and E.L. Turner, Mon. Not. R. Astr. Soc. **259**, 421 (1992).
126. M.A. Malkan, *Structure and Emission Properties of Accretion Disks*, eds. C. Bertout, S. Collin-Souffrin, J.P. Lasota and J. Tran Thanh Van (Editions Frontiers, 1991), p. 165.
127. J.P.D. Mittaz and G. Branduardi-Raymont, Mon. Not. R. Astr. Soc. **238**, 1029 (1989).
128. F. Fiore, E. Massaro and P. Barone, Astron. Astrophys. **261**, 405 (1992).
129. C. Done, G.M. Madejski, R.F. Mushotzky, T.J. Turner, K. Koyama and H. Kunieda, Astrophys. J. **400**, 138 (1992).
130. F.H. Wallinder, S. Kato and M.A. Abramowicz, Astron Astrophys. Rev. **4**, 79 (1992).
131. M.A. Abramowicz, A. Lanza, E.A. Spiegel and E. Szuszkiewicz, Nature **356**, 41 (1992).
132. M.A. Abramowicz, G. Bao, F. Fiore, E. Massaro, G.C. Perola, E.A. Spiegel and E. Szuszkiewicz, *Physics of Active Galactic Nuclei*, eds. W.J. Duschl and S.J. Wagner (Springer-Verlag, 1992).
133. M.J. Rees (1992, personal communication).
134. D. Syer, C.J. Clarke and M.J. Rees, Mon Not. R. Astr. Soc. **250**, 505 (1991).
135. W.H. Zurek, A. Siemiginowska and S.A. Colgate, *Testing the AGN Paradigm*, eds. S.S. Holt, S.G. Neff and C.M. Urry, AIP Conf. No. 254 (1992), p. 564.
136. C. Done, G.M. Madejski, R.F. Mushotzky, T.J. Turner, K. Koyama and H. Kunieda, *Frontiers of X-ray Astronomy*, ed. Y. Tanaka (Universal Academy Press, Tokyo, 1992).
137. S. Tsuruta, *The Nature of Compact Objects in AGN* (Cambridge University Press, in preparation).
138. C. Done and A.R. King (1993, in preparation).
139. F.H. Wallinder, *The Nature of Compact Objects in AGN* (Cambridge University Press, in preparation).
140. F. Honma, R. Matsumoto and S. Kato, Publ. Astron. Soc. Japan **44**, 529 (1992).
141. M.A. Nowak and R.V. Wagoner, Astrophys. J. **378**, 656 (1991).

Contents Previous